



# Dissolution mechanism of supported phospholipid bilayer in the presence of amphiphilic drug investigated by neutron reflectometry and quartz crystal microbalance with dissipation monitoring

V. Foroqi Motlaq<sup>a,b,1</sup>, F.A. Adlmann<sup>a,b,1</sup>, V. Agmo Hernández<sup>a</sup>, A. Vorobiev<sup>c</sup>, M. Wolff<sup>c</sup>, L.M. Bergström<sup>a,b,\*</sup>

<sup>a</sup> Department of Medicinal Chemistry, Uppsala University, P.O. Box 547, 751 23 Uppsala, Sweden

<sup>b</sup> Department of Pharmacy, Uppsala University, P.O. Box 580, 75123 Uppsala, Sweden

<sup>c</sup> Division for Materials Physics, Department of Physics and Astronomy, Uppsala University, Box 516, 751 20 Uppsala, Sweden

## ARTICLE INFO

### Keywords:

Lipid bilayer  
Phospholipid  
DOPC  
Amitriptyline  
Neutron reflectometry  
Amphiphilic drug  
Membrane transport  
Membrane solubilization  
SLB

## ABSTRACT

The influence and interaction of the ionizable amphiphilic drug amitriptyline hydrochloride (AMT) on a 1,2-dioleoyl-sn-glycero-3-phosphocholine (DOPC) phospholipid bilayer supported on a silica surface have been investigated using a combination of neutron reflectometry and quartz crystal microbalance with dissipation monitoring. Adding AMT solutions with concentrations 3, 12, and 50 mM leaves the lipid bilayer mainly intact and we observe most of the AMT molecules attached to the head-group region of the outer bilayer leaflet. Virtually no AMT penetrates into the hydrophilic head-group region of the inner leaflet close to the silica surface. By adding 200 mM AMT solution, the lipid bilayer dissolved entirely, indicating a threshold concentration for the solubilization of the bilayer by AMT. The observed threshold concentration is consistent with the observation that various bilayer structures abruptly transform into mixed AMT-DOPC micelles beyond a certain AMT-DOPC composition. Based on our experimental observations, we suggest that the penetration of drug into the phospholipid bilayer, and subsequent solubilization of the membrane, follows a two-step mechanism with the outer leaflet being removed prior to the inner leaflet.

## 1. Introduction

Phospholipids are the main component responsible for the formation of bilayer membranes and have been an important subject of studies for decades [1–3]. The membranes are usually very stable but may be disrupted and dissolved by amphiphilic surface-active molecules. An important class of amphiphilic molecules with surfactant properties is amphiphilic drugs, which are known to interact and self-assemble with phospholipid bilayers and influence properties related to pharmacological activity and toxicity [4–7]. Amphiphilic drugs differ in chemical structure from conventional surfactants in the sense that they are usually composed of a rather rigid hydrophobic part attached to a head group. In this respect, amphiphilic drugs are similar to another, from a biological perspective, important class of amphiphilic molecules, bile salts. Bile salt surfactants are extraordinarily effective in dissolving phospholipids into mixed micelles, which may have a phospholipid content as high as

70–85% [8,9]. Amphiphilic drugs appear to have somewhat lower ability to dissolve phospholipids than bile salts, but significantly larger ability than conventional surfactants. Amphiphilic drugs, and the chemically similar class of bile salt surfactants, share a property of significantly higher spontaneous curvature than conventional surfactants. This makes amphiphilic drugs and bile salts particularly effective in breaking up bilayer membranes and solubilizing substantial amounts of phospholipids into mixed micelles. The molecular interaction between drugs and phospholipid membranes is expected to be crucial for the performance of the drug.

Tricyclic anti-depressants are amphiphilic molecules that consist of a rigid hydrophobic tail and small hydrophilic head group that can self-assemble and form small micelles above the critical micelle concentrations (CMC) [5,10]. The tricyclic anti-depressant amitriptyline (AMT) is a psychoactive drug that is mainly used for two medical applications [11]. It is a non-selective reuptake inhibitor, which interacts on the

\* Corresponding author at: Uppsala University, Biomedicinskt Centrum BMC, Box 574, 751 23 Uppsala, Sweden.

E-mail address: [magnus.bergstrom@ilk.uu.se](mailto:magnus.bergstrom@ilk.uu.se) (L.M. Bergström).

<sup>1</sup> Both authors contributed equally.

carriers in the synaptic cleft to inhibit the synaptic reuptake of serotonin, dopamine, and noradrenalin to treat depression. The effect is enhanced after an adjustment period due to a change in receptor sensitivity caused by the shift in concentration. As a painkiller for suddenly occurring neuropathic pain, AMT prevents non-physiological action potentials (use dependency) by reversibly blocking fast reacting sodium channels. A similar process is described for potassium channels. The substance must be incorporated into the membrane in order to trigger this kind of physiological response [12–15]. For this mechanism, Sheetz and Singer formulated their bilayer couple hypothesis suggesting that the two halves of the membrane could respond differently to perturbations while remaining coupled to each other [16]. In addition, it has been shown the same interaction between drug and phospholipid membrane leads to AMT having properties of an anesthetic [17,18]. To investigate the dynamics in the system a time estimate ( $5.64 \times 10^{-3} \text{ s}^{-1}$ – $5.28 \times 10^{-8} \text{ s}^{-1}$  at 20 °C) for the so-called flip-flop, i.e. the transfer from one bilayer leaflet to the other, was determined [19–21]. Similar values for flip-flop rates in membranes were obtained for gramicidin [22,23].

Neutron scattering techniques offer several unique opportunities to study structure and dynamics due to molecular interactions in bilayers composed of more than one component. Especially selective deuteration opens possibilities to observe the behavior of living material by making some parts visible. The unique ability of neutrons to be truded to the surface through silicon makes neutron reflectivity an excellent tool to investigate interfaces and supported bilayers [24]. Neutron reflectometry (NR) studies of supported bilayers with inserted helical peptides [25], cubosomes [26], quinolone antibiotics [27], antimicrobial peptides [28], triphosphates [29], and, lipoproteins [30] have been reported recently. In particular, the effect of antimicrobial agents on bilayer properties has been investigated and characterized [31].

Other surface sensitive techniques to investigate supported bilayers include quartz crystal microbalance with dissipation monitoring (QCM-D) [32,33]. QCM-D allows monitoring changes in the mass and viscoelastic properties of immobilized films, and can be used to monitor the binding of small molecules to lipid bilayer based structures and to characterize the effect of these insertions into the membrane properties [34–36].

In the present work, we combine neutron reflectometry and QCM-D to study the molecular distribution, and the eventual membrane break-up and dissolution, when adding an amphiphilic drug to a one-component phospholipid model membrane. We have chosen the phosphatidylcholine 1,2-dioleoyl-sn-glycero-3-phosphocholine (DOPC) as phospholipid. DOPC has a gel-to-liquid crystalline transition temperature equal to  $T_c = -22 \text{ °C}$  and is known to form a fluid, stable and homogenous lipid bilayer at room temperature [37]. As a result, we are able to locate the drug molecules mainly to the outer leaflet of the supported bilayer and observe the final membrane dissolution in a two-step process above a threshold concentration of drug.

## 2. Experimental details

### 2.1. Materials and sample procedure

Synthetic hydrogenous DOPC (1,2-dioleoyl-sn-glycero-3-phosphocholine) was purchased from Larodan's research grade lipids. Tail-deuterated  $d_{64}$ -DOPC was purchased from Frankenstein Bio Reagents (FB Reagents) and amitriptyline (AMT) from Sigma-Aldrich. All chemicals were used as received without further purification. The glasswares for sample preparation have been immersed overnight in 2% Hellmanex III solution followed by extensive rinsing first with MilliQ water, followed by pure ethanol. The chemical structures of DOPC and AMT are displayed in Fig. 1.

The supported lipid bilayers (SLB) for both NR and QCM-D were deposited through the fusion of tip-sonicated vesicles, and details of the procedure can be found elsewhere [38,39]. Briefly, the phospholipid was dissolved in chloroform and the solvent was evaporated in a rotary evaporator. Traces of solvent were removed under vacuum overnight. The phospholipid films were stored at  $-20 \text{ °C}$  and prior to the experiment hydrated with 50 mM sodium fluoride solution and vortexed for 5 min.

The emerging solution containing the lipid bilayers was sonicated to form small vesicles (25–35 nm, as measured by DLS). Centrifuging was used to remove titanium debris from the tip-sonication. The dispersion was then loaded into the measurement cell where the liposomes come in contact with UV/ozone treated surface and spontaneously ruptured and formed a supported lipid bilayer on top of the used silica substrates. It is in agreement with previous reports and our own observations (see results section). Once formed the NaF buffer was replaced with MilliQ water for the QCM-D and heavy water for the NR measurements.

The samples in the text below are denoted with a letter “H” or “D”, which indicates whether the SLB is hydrogenous or tail-deuterated. The letter is followed by a number referring to the concentration of AMT that is injected, i.e. H0, H3, H12, H50, and H200 for 0, 3, 12, 50, and 200 mM, respectively.

### 2.2. Quartz crystal microbalance with dissipation monitoring

The QCM-D measurements were carried out on the Q-Sense QCM-D connected with an E1 module (Q-Sense, Gothenburg, Sweden) connected to a peristaltic pump. Commercially available silica-coated sensors (Q-sense, Gothenburg, Sweden) were used. The fundamental frequency of 4.95 MHz as well as 3th, 5th, 7th, 9th, 11th, and 13th overtones were monitored and 3th–13th was used for mass calculation in this study. The sensors were cleaned using the procedure recommended by the producer, shortly, the sensors were treated in a UV/ozone chamber for 10 min, then immersed in SDS (2% solution) for 20 min, then 10 min in MilliQ water, followed by extensive rinsing with water and ethanol and dried with gentle nitrogen flow. Finally, prior to use, the sensors were exposed again 20 min in UV/ozone chamber ensuring the formation of a clean and hydrophilic surface. All experiments were performed at 21 °C, starting with the injection of NaF 50 mM buffer [40,41], after establishing a flat baseline, the liposome, in the

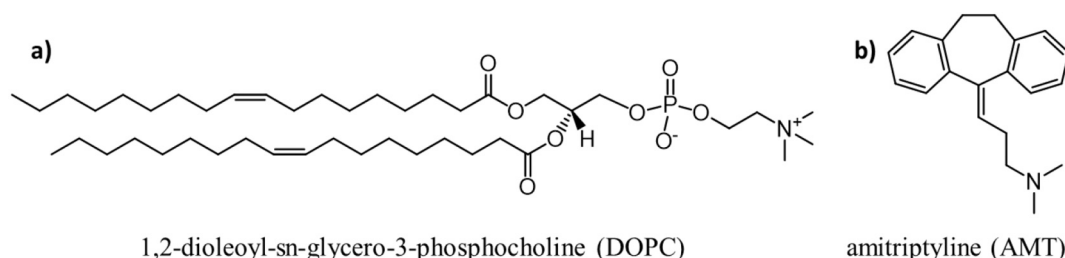


Fig. 1. Structural chemical formulas of (a) DOPC and (b) AMT.

same buffer, was introduced to the system. During the bilayer formation steps of each experiment liposomes were injected at a flow rate of  $150 \mu\text{L min}^{-1}$ . Spontaneous rupture of liposomes due to the interaction with the hydrophilic silica surface results in the formation of the supported phospholipid bilayer. After SLB formation, the remaining intact liposomes were removed by rinsing with buffer and, finally, MilliQ water. Subsequently, for the SLB-drug interaction experiment, the flow rate was decreased to  $15 \mu\text{L min}^{-1}$ .

### 2.2.1. QCM-D modelling

The immobilized mass on the QCM-D sensor, for a rigid and comparably thin adsorbed layer (i.e. for a negligible change in the dissipation factor, i.e.  $\Delta D \approx 0$ ) can be calculated through the Sauerbrey equation [42]:

$$\Delta m = \frac{\Delta f_n}{n} C$$

where  $\Delta m$  is mass per unit area adsorbed on the sensor,  $\Delta f_n$  is the shift in oscillation frequency,  $n$  is the corresponding overtone, and  $C$  is  $17.7 \text{ ng/cm}^2 \text{ Hz}^{-1}$  for a 4.95 MHz sensors crystal. In order to be able to use the Sauerbrey equation, the collected data were corrected for "bulk effect" through a process proposed by Höök et al. [43]. Briefly, it was assumed that changes in dissipation were only related to changes in the density and viscosity of the medium and not to the immobilized layer, a fair assumption considering that the dissipation from SLBs is very close to zero [42]. Under these conditions, the frequency changes associated with changes in the medium can be calculated and subtracted from the recorded signal. The Sauerbrey equation is then valid if the resultant corrected signals overlap for all overtones (indicating the formation of a rigid layer).

### 2.3. Neutron reflectometry

The reflectometry experiment was conducted at the reflectometer SuperADAM (Institute Laue-Langevin, Grenoble, France) [44]. A  $q$  range between 0 and  $0.15 \text{ \AA}^{-1}$  was measured. SuperADAM uses a wavelength of  $5.215 \text{ \AA}$  with a resolution of 0.4%. Both slits in the incident beam were set to 1 mm and kept constant throughout the whole experiment. To investigate molecular interactions mechanisms at the interface, the off-specular signal is taken automatically by the usage of a position-sensitive detector and multiple regions of interest. In none of the data sets off specular signal beyond noise was detected, which shows good layer formation. Background reduction and direct beam normalization as well as the over-illumination correction were done by the software pySAred [45].

Small vesicle fusion was chosen as the method to form the supported phospholipid bilayer in order to minimize the risk to manipulate the substrate during the mounting process and avoid having it dewetted. Similar to the liposome collapse described in [46], liposomes were prepared in 50 mM sodium fluoride in  $\text{D}_2\text{O}$  and then filled into the sample cell. The cell was filled slowly, i.e.  $1 \text{ cm}^3 \text{ min}^{-1}$ , the buffer replaced with pure heavy water, and consequently, filled with a different mixture of AMT in heavy water.

#### 2.3.1. Neutron reflectometry modelling

Specular neutron reflectometry measures the intensity, which is reflected from an interface versus momentum transfer  $q_z$  of the neutron perpendicular to that interface. From the data, information is obtained about the scattering length density (SLD) profile across the interface or layered structures. The SLD is calculated from the number density  $n_i$  and the bound coherent scattering length for neutrons  $b_i$  of the respective nuclei, according to:

$$SLD = \sum_i (n_i b_i)$$

Note  $b_i$  for the two isotopes, hydrogen and deuterium, are very

different allowing labeling and contrast variation experiments to determine the location of individual molecular components in a bilayer. The SLDs of the key components for the present study are summarized in Table S1 in the Supplementary data.

The data analysis was done with GenX [47], which uses differential evolution (DE) a genetic algorithm for fitting. We chose chi-square as a figure of merit, FOM. For further details, we refer to literature [48]. The data were fitted with a four-layer model representing the outer and inner parts of the lipid membrane to extract SLD profiles.

## 3. Results and discussion

### 3.1. Quartz crystal microbalance experiment

In order to study the DOPC bilayer and different concentrations of amitriptyline solution, the formation of a DOPC bilayer was confirmed. Fig. 2.a shows the surface mass density accumulated on the QCM-D sensors as a function of time, calculated as described in the methods section. An increase in both frequency and dissipation due to an initial immobilization of intact liposomes followed by a decrease in both parameters upon vesicle rupture is evident in Fig. 2.a. Unreacted and loosely attached liposomes were removed by rinsing with buffer (NaF), and finally, MilliQ water. The final frequency shift of  $\sim 25 \text{ Hz}$  and low dissipation values are very close to previously reported values [49], suggesting the formation of a supported continuous DOPC bilayer.

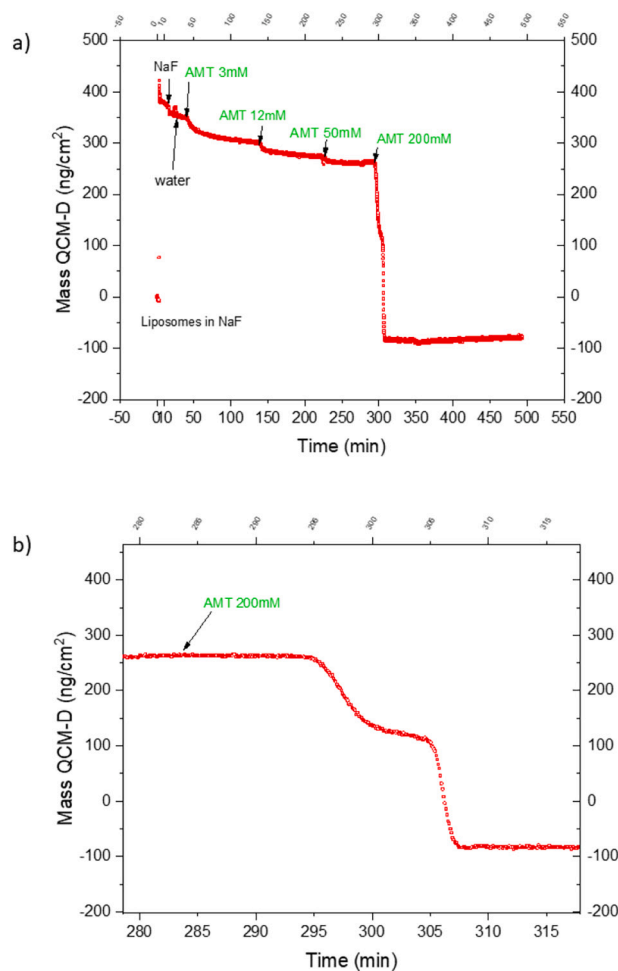


**Fig. 2.** a) Bulk effect corrected immobilized mass of QCM-D experiment of four different concentration (3, 12, 50, and 200 mM) of amitriptyline introduced to the supported DOPC bilayer. b) The enlargement part of the curve after 200 mM amitriptyline solution injected.

After establishing the DOPC bilayer, the lowest amitriptyline concentration (3 mM) was introduced with a flow rate of  $15 \mu\text{L min}^{-1}$ . A slight decrease in the immobilized mass was observed, indicating partial solubilization of the bilayer. The consecutive injection of 12 and 50 mM amitriptyline followed the trend, by increasing the amitriptyline concentration, more bilayer detached from the sensor's surface. Interestingly, after equilibration with a solution of 50 mM AMT, which is above its critical micelle concentration (CMC  $\approx 37$  mM), most of the bilayer remained immobilized, indicating that this concentration was not enough to remove the whole bilayers.

In the case of 200 mM, i.e. about 5 times CMC, the QCM-D profile illustrates that the amitriptyline concentration is sufficient to dissolve the DOPC bilayer entirely in a two-step process. After the addition of the AMT solution, a sudden drop in immobilized mass is observed. The mass is then stabilized for a few minutes before dropping abruptly again. The enlarged QCM-D curve after injection of 200 mM AMT is depicted in Fig. 2.b and a shoulder in the curve can be observed. The change in immobilized mass is roughly the same in each of the steps. The results suggest the scenario in which amitriptyline dissolves the top and bottom monolayers of the bilayer in two separate steps.

To verify this effect for an intact DOPC bilayer, a 200 mM amitriptyline solution was infused into a fresh DOPC bilayer. The resulting surface mass density profile is depicted in Fig. 3. It is evident that the same interaction as described above is still dominant: 200 mM solution of amitriptyline completely dissolves the DOPC bilayer in a two-step process. On the right hand side of the same graph, the standard deviation of the different bulk corrected overtones (f3-f13) is shown. As AMT introduced to the SLB the standard deviation of the different bulk corrected overtones (STD) increases dramatically, indicating that the Sauerbrey equation is no longer valid and suggesting that a viscoelastic film replaces the rigid bilayer.

Interestingly, the standard deviation of the different bulk corrected overtones drops at 38 min, sharply right after the moment where the second dissolution step begins (implying that the film becomes more rigid) and then increases again, suggesting a softening of the film. This drop happens at half of the initial surface density mass on the sensor. This indicates that each leaflet has been dissolved separately and can be explained as follows: at 200 mM a sufficient amount of AMT penetrates into the outer leaflet of the bilayer solubilizing it by forming mixed micelles that remain close to the oppositely charged surface, contributing to a higher dissipation factor. The consequent drops of STD when AMT incorporates into the inner leaflet, indicating a rigid film exists for

a few seconds right before the leaflet is solubilized into mixed micelles. It is interesting to note that the solubilization of the inner leaflet is faster than the first step, which might be due to the fact that after removing the top layer the hydrocarbon tails of DOPC initially come in direct contact with water which is unfavorable.

It is to be noted, that after the addition of the 200 mM AMT solution the corrected signals do not overlap for the different overtones (c.f. Supplementary data S.I.), resulting in the large STD mentioned above and, suggesting that the underlying assumption, meaning the rigidity of the layer on the sensor, is no longer valid and the immobilized film is no longer rigid. It is also to be noted that the final mass values determined after solubilization in the experiments discussed above are negative, which has no physical meaning. The fact that the "bulk effect" for the final part of the QCM-D curves, where most of the bilayer has been removed, cannot be corrected according to the procedure described in the method section, advocates the idea that adding a 200 mM amitriptyline solution leads to the spontaneous dissolution of the bilayer and leaves the surface of the sensor with a viscoelastic layer. We believe that this is related to the fact that the AMT concentration has reached and exceeded the limit where AMT may dissolve the phospholipid to form AMT-rich mixed micelles that remain close to the interface with the opposite charge. This idea has been examined by injection of 200 mM amitriptyline to the naked silica surface and a similar QCM-D profile was observed (c.f. Supplementary data S.II.) as for the final stage of the experiments with the bilayer. This behavior was also supported by neutron reflectometry as discussed below.

The observed threshold where the SLB is completely dissolved by an AMT solution as concentrated as five times the critical micelle concentration is consistent with bulk observations of a rather abrupt transition from bilayer aggregates to small micelles at a mole fraction of DOPC  $X_{PL} = 0.35$  in the aggregates (unpublished data).

### 3.2. Neutron reflectometry experiment

To unveil the mechanisms of lipid bilayer-drug interaction, we have complemented our QCM-D experiments with neutron reflectometry. To distinguish between drug substitution and membrane dissolution, the experiment is performed using both a hydrogenous and a deuterated phospholipid.

Fig. 4 shows the NR experimental data, as well as the scattering length densities (SLD) profiles, obtained from our data analysis. In the SLD profiles,  $z = 0$  indicates the surface of the silicon substrate. It is evident from all our neutron data, particularly for samples with hydrogenous SLB, that there is a thin layer of water between the silica surface and the lipid bilayer. Head groups and water mix and it was not possible to distinguish between the inner head group and the water layer. Therefore we allowed for one inner layer composed of both inner head groups and surface water in our data analysis. We have determined the mean thickness of the SLB is about 40 Å, which agrees with the previously reported value of 38 Å for the DOPC bilayer [46,50].

Fig. 5 shows the SLD profile of an intact hydrogenous and tail-deuterated DOPC bilayer, before and after injection of 3 mM AMT solution. Both profiles show a reduced SLD in the region of the outer head group. From the experiments with hydrogenous and deuterated phospholipid, we calculated the concentration of each compound in the bilayer, i.e. AMT, water, and DOPC. The inset in Fig. 5 shows the mole percent of AMT and water in the bilayer plotted against the bilayer profile thickness ( $z$ ). The drug is incorporated in the outer bilayer leaflet at low AMT concentrations. The SLD change indicates changes in composition in the bilayer. It is evident that AMT has a high affinity to the phospholipid head group region and almost all of it accumulates near the outer edge of the SLB where head groups are in contact with a free solution. The other notable feature in Fig. 5 is the increase of total SLD of the head and chain region in the sample 3 mM AMT. This is because the addition of AMT leads to an increase in the amount of water ( $\text{D}_2\text{O}$  in this case) and, consequently, an increase of the total SLD in both

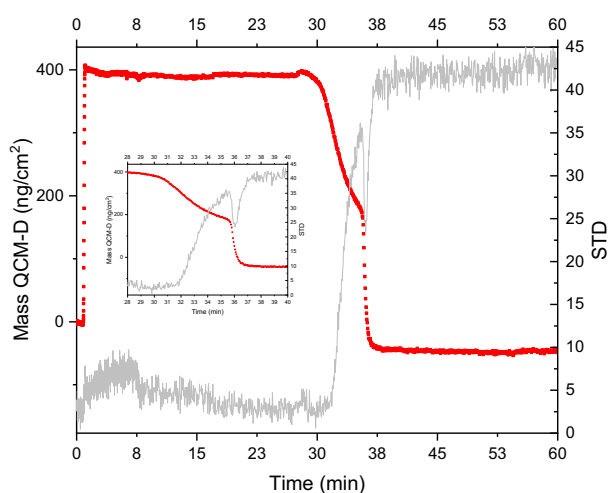
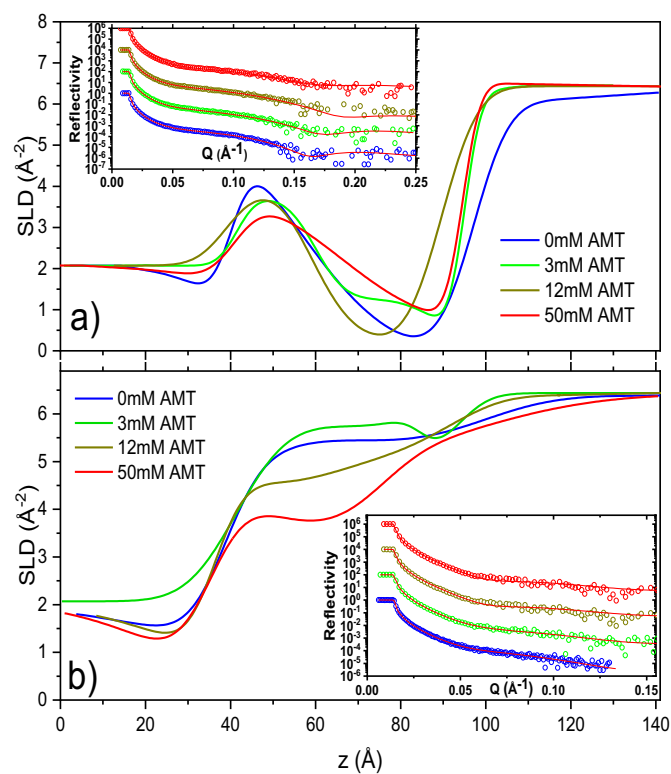
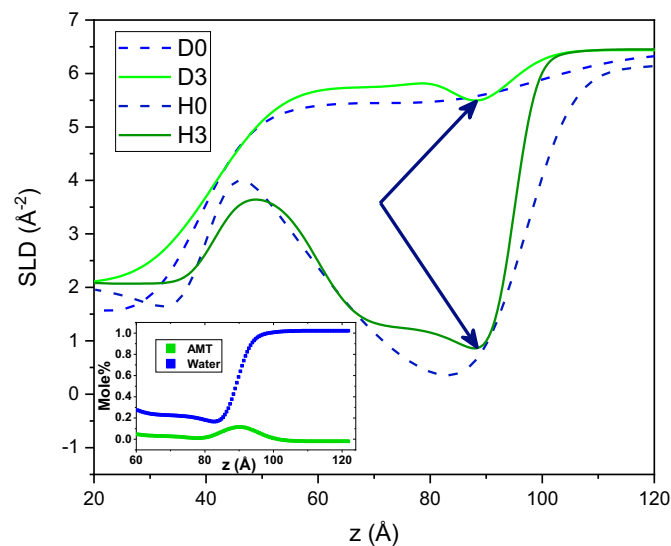


Fig. 3. Bulk effect corrected immobilized mass of QCM-D experiment of 200 mM amitriptyline solution infused to an intact supported DOPC bilayer. On the right, Y-axis shows the standard deviation of the different overtone (f5-f11) after bulk correction. The inset plot magnifies the solubilization range.





**Fig. 4.** Illustration of the different scattering length density (SLD) profiles resulting from iterative fit analysis of DOPC bilayer exposed to different concentration of amiriptryline (3, 12, and 50 mM AMT); a) hydrogenous DOPC and b)  $d_{64}$ -DOPC bilayer. Blue line shows the first experiment of pure bilayer. The inset plots show the corresponding NR experiments. The red solid line shows the fit for each data set. The decade offset in the inset inlay is used for visualization purposes.



**Fig. 5.** Illustration of the different scattering length density (SLD) profiles resulting from iterative fit analysis of hydrogenous as well as tail-deuterated intact DOPC bilayer (dashed lines), and after exposure to 3 mM amiriptryline (solid lines). It shows high affinity of AMT for the outer head groups.

regions.

In QCM-D, we observe a slight decrease in the total mass of SLB after injection of 12 mM AMT solution. Density calculations show that 33% of

SLB in the outer head-group region consists of AMT and that the total amount of water in the SLB increases after incorporation of AMT in the SLB. From this, we conclude that AMT replaces DOPC molecules when incorporated into the bilayer. Since AMT is an amphiphilic molecule, which is more hydrophilic than DOPC, a larger amount of water is incorporated along with AMT into the interface region. The addition of AMT and water almost compensates for the loss of DOPC molecules.

Our QCM-D measurements revealed that the adsorbed mass was reduced upon increasing AMT concentration, which is consistent with patches of phospholipid being dissolved in the solution. Table 1 shows the amount of AMT and water in the various bilayer regions for each concentration of injected AMT solution. As the AMT concentration increases, AMT penetrates deeper into the bilayer and the amount of AMT incorporated in the inner tail and head group regions increases. Moreover, the increase in the fraction of water in the inner leaflet region indicates that the structure of the SLB layer has become perturbed, and the organized phospholipid bilayer has started to become dissolved into the bulk in the form of mixed AMT-DOPC micelles. This is in agreement with QCM-D data shown in Fig. 2 as well as with previous findings indicating that the addition of AMT decrease the acyl chain order in liposomes formed by the phospholipid DMPC [51].

The resultant SLD after the addition of 200 mM solution of the AMT to d-DOPC and h-DOPC bilayer is shown in Fig. 6. The NR profile fits suggest that the SLB has been removed completely. The slightly reduced SLD may be explained by the formation of a new layer of mixed AMT-DOPC micelles on the silica surface. This hypothesis is supported by comparing with the SLD profile when injecting 200 mM AMT to the bare UV/ozone silicon wafer (cf. Fig. 2). This result is in good agreement with our QCM-D data, and the observation of a new viscoelastic layer replacing the SLB. Although, the concentration above CMC severely perturbed the bilayer and its structural order, a concentration as high as five times the CMC was needed to entirely dissolve the bilayer.

#### 4. Conclusion

The penetration of the amphiphilic drug amiriptryline hydrochloride (AMT) into, and the subsequent dissolution of, a supported DOPC phospholipid bilayer (SLB) have been studied by a combination of quartz crystal microbalance with dissipation monitoring (QCM-D) and neutron reflectometry (NR). The QCM-D results show that the complete dissolution of the SLB occurs at a drug concentration threshold about five times the critical micelle concentration of AMT ( $\sim 200$  mM). This observation agrees with our NR experiments, according to which no sign of SLB could be observed after addition above a threshold of about  $[\text{AMT}] = 200$  mM. The complete removal of the SLB above a threshold concentration of the drug is consistent with our observations in bulk solution of an abrupt transition from bilayer aggregates to rather small mixed AMT-DOPC micelles at a mole fraction of about  $x_{PL} = 0.35$ .

Moreover, the QCM-D results demonstrate that solubilization of the membrane is a two-step process where AMT solubilizes each bilayer leaflet separately. This is consistent with our NR experiments, which indicate a high affinity of AMT in the outer head group region, and a low tendency of the drug to penetrate deep into the bilayer. After removal of the phospholipid bilayer, both NR and QCM-D results suggest that a new viscoelastic layer is formed over the silica surface, consistent with the formation of mixed AMT-DOPC mixed micelles loosely attached to the oppositely charged surface.

Our study demonstrates the strength of the combination of QMCD and NR techniques and gives new insights to the processes of membrane penetration, which is, relevant when studying the therapeutic effect of AMT sodium (and potassium) channel blockage, and ultimate dissolution of phospholipids by amphiphilic drugs, for instance. Future experiments could include a kinetic study of the membrane effects, which, however, requires significantly higher neutron flux than available in the present study.

**Table 1**

Amitriptyline and water content in different part of SLB before and after injection of three different concentrations of amitriptyline (3, 12, and 50 mM AMT).

Injected AMT concentration	0 (SLB)		3 mM		12 mM		50 mM	
	AMT [%]	Water [%]	AMT [%]	Water [%]	AMT [%]	Water [%]	AMT [%]	Water [%]
Inner head	–	28	10	28	33	38	46	40
Chain	–	11	3	23	28	33	48	40
Upper head	–	15	11	10	11	7	18	13

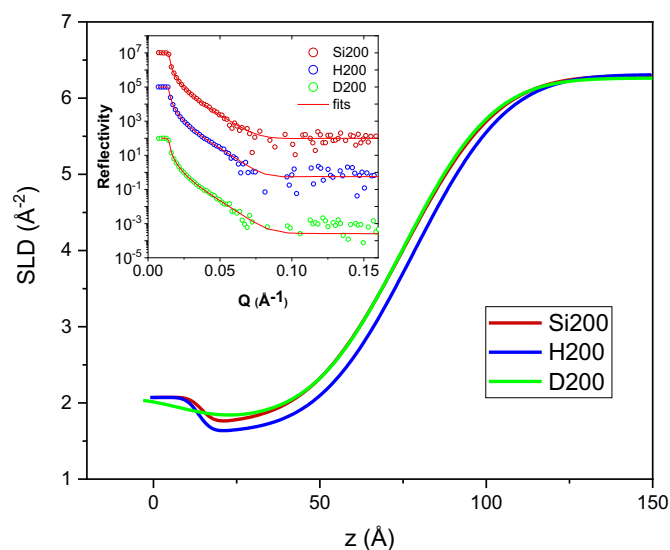


**Fig. 6.** Illustration of the different scattering length density (SLD) of hydrogenous (H200) and tail-deuterated (D200) DOPC bilayer as well as pure silicon substrate (Si200) exposed to 200 mM amitriptyline. The inset plot shows the corresponding NR experiments. The red solid line shows the fit for each data set. The decade offset in the inset inlay is used for visualization purposes.

### Declaration of competing interest

The authors declare that they have no known competing financial interests or personal relationships that could have appeared to influence the work reported in this paper.

### Acknowledgments

This study is part of the science programs of the Swedish Drug Delivery Forum (SDDF) and the Swedish Drug Delivery Center (SweDeliver) with financial support from Vinnova (Dnr 2017-02690 and Dnr 2019-00048, respectively). We are also grateful to the Faculty of Pharmacy at Uppsala University for financial support. The authors acknowledge the help of Sana Tirgani during the sample preparation, V. Gelev from FBreagents, Olivier Aguetz for his help during the reflectometry measurement, and Katarina Edwards for providing access to the QCM-D instrument as well as the Institute Laue Langevin for providing beam time. We also acknowledge the Swedish Research Council for financial support of the SuperADAM project.

### Appendix A. Supplementary data

Supplementary data to this article can be found online at <https://doi.org/10.1016/j.bbmem.2022.183976>.

### References

- [1] M. Almgren, Mixed micelles and other structures in the solubilization of bilayer lipid membranes by surfactants, *Biochim. Biophys. Acta Biomembr.* 1508 (1) (2000) 146–163.
- [2] M. Almgren, Vesicle transformations resulting from curvature tuning in systems with micellar, lamellar, and bicontinuous cubic phases, *J. Dispers. Sci. Technol.* 28 (1) (2007) 43–54.
- [3] M. Almgren, Stomatosomes: perforated bilayer structures, *Soft Matter* 6 (7) (2010) 1383–1390.
- [4] A. Sosnik, Drug self-assembly: a phenomenon at the nanometer scale with major impact in the structure–biological properties relationship and the treatment of disease, *Prog. Mater. Sci.* 82 (2016) 39–82.
- [5] D. Attwood, The mode of association of amphiphilic drugs in aqueous solution, *Adv. Colloid Interf. Sci.* 55 (1995) 271–303.
- [6] S. Schreier, S.V.P. Malheiros, E. de Paula, Surface active drugs: self-association and interaction with membranes and surfactants. Physicochemical and biological aspects, *Biochim. Biophys. Acta Biomembr.* 1508 (1) (2000) 210–234.
- [7] P. Seeman, The membrane actions of anesthetics and tranquilizers, *Pharmacol. Rev.* 24 (4) (1972) 583–655.
- [8] A. Hildebrand, et al., Bile salt induced solubilization of synthetic phosphatidylcholine vesicles studied by isothermal titration calorimetry, *Langmuir* 18 (7) (2002) 2836–2847.
- [9] V. Foroqi Motlaq, et al., Investigation of the enhanced ability of bile salt surfactants to solubilize phospholipid bilayers and form mixed micelles, *Soft Matter* 17 (33) (2021) 7769–7780.
- [10] C. Efthymiou, et al., Self-assembling properties of ionisable amphiphilic drugs in aqueous solution, *J. Colloid Interface Sci.* 600 (2021) 701–710.
- [11] J. Moraczewski, K.K. Aedma, Tricyclic antidepressants, in: StatPearls [Internet], StatPearls Publishing, 2020.
- [12] T. Horishita, et al., Antidepressants inhibit Nav1.3, Nav1.7, and Nav1.8 neuronal voltage-gated sodium channels more potently than Nav1.2 and Nav1.6 channels expressed in *Xenopus* oocytes, *Naunyn Schmiedeberg's Arch. Pharmacol.* 390 (12) (2017) 1255–1270.
- [13] T.A. Atkin, et al., A comprehensive approach to identifying repurposed drugs to treat SCN8A epilepsy, *Epilepsia* 59 (4) (2018) 802–813.
- [14] C. Nau, et al., Block of human heart hH1 sodium channels by amitriptyline, *J. Pharmacol. Exp. Ther.* 292 (3) (2000) 1015–1023.
- [15] M.A. Punke, P. Friederich, Amitriptyline is a potent blocker of human Kv1.1 and Kv7.2/7.3 channels, *Anesth. Analg.* 104 (5) (2007).
- [16] M.P. Sheetz, S.J. Singer, Biological membranes as bilayer couples. A molecular mechanism of drug-erythrocyte interactions, *Proc. Natl. Acad. Sci.* 71 (11) (1974) 4457.
- [17] N. Kitagawa, et al., A proposed mechanism for amitriptyline neurotoxicity based on its detergent nature, *Toxicol. Appl. Pharmacol.* 217 (1) (2006) 100–106.
- [18] R. Salimi, et al., Local anesthetic effect of amitriptyline versus lidocaine in isolated lesion of the limb requiring primary suturing; assessing a novel therapeutic agent, *Bull. Emerg. Trauma* 7 (3) (2019) 240–244.
- [19] M.S. Bretscher, Asymmetrical lipid bilayer structure for biological membranes, *Nat. New Biol.* 236 (61) (1972) 11–12.
- [20] A.A. Gurtovenko, I. Vattulainen, Molecular mechanism for lipid flip-flops, *J. Phys. Chem. B* 111 (48) (2007) 13554–13559.
- [21] J.S. Allhusen, J.C. Conboy, The ins and outs of lipid flip-flop, *Acc. Chem. Res.* 50 (1) (2017) 58–65.
- [22] H. Tournois, et al., Relationship between gramicidin conformation dependent induction of phospholipid transbilayer movement and hexagonal HII phase formation in erythrocyte membranes, *Biochim. Biophys. Acta Biomembr.* 946 (1) (1988) 173–177.
- [23] N.C. Santos, J. Martins-Silva, C. Saldanha, Gramicidin D and dithiothreitol effects on erythrocyte exovesiculation, *Cell Biochem. Biophys.* 43 (3) (2005) 419–430.
- [24] J. Penfold, R.K. Thomas, The application of the specular reflection of neutrons to the study of surfaces and interfaces, *J. Phys. Condens. Matter* 2 (6) (1990) 1369–1412.
- [25] M.B. Smith, et al., Neutron reflectometry of supported hybrid bilayers with inserted peptide, *Soft Matter* 6 (5) (2010) 862–865.
- [26] L. Boge, et al., Peptide-loaded cubosomes functioning as an antimicrobial unit against *Escherichia coli*, *ACS Appl. Mater. Interfaces* 11 (24) (2019) 21314–21322.
- [27] A.T.M. Hubbard, et al., Mechanism of action of a membrane-active quinoline-based antimicrobial on natural and model bacterial membranes, *Biochemistry* 56 (8) (2017) 1163–1174.
- [28] R. Rehal, et al., The pH-dependence of lipid-mediated antimicrobial peptide resistance in a model staphylococcal plasma membrane: a two-for-one mechanism of epithelial defence circumvention, *Eur. J. Pharm. Sci.* 128 (2019) 43–53.
- [29] A. Luchini, et al., Towards biomimics of cell membranes: structural effect of phosphatidylinositol triphosphate (PIP3) on a lipid bilayer, *Colloids Surf. B: Biointerfaces* 173 (2019) 202–209.
- [30] K.L. Browning, et al., Effect of bilayer charge on lipoprotein lipid exchange, *Colloids Surf. B: Biointerfaces* 168 (2018) 117–125.

- [31] B. Bechinger, The structure, dynamics and orientation of antimicrobial peptides in membranes by multidimensional solid-state NMR spectroscopy, *Biochim. Biophys. Acta Biomembr.* 1462 (1) (1999) 157–183.
- [32] C.A. Keller, B. Kasemo, Surface specific kinetics of lipid vesicle adsorption measured with a quartz crystal microbalance, *Biophys. J.* 75 (3) (1998) 1397–1402.
- [33] N.-J. Cho, et al., Quartz crystal microbalance with dissipation monitoring of supported lipid bilayers on various substrates, *Nat. Protoc.* 5 (6) (2010) 1096–1106.
- [34] G.A. McCubbin, et al., QCM-D fingerprinting of membrane-active peptides, *Eur. Biophys. J.* 40 (4) (2011) 437–446.
- [35] V. Agmo Hernández, K. Reijmar, K. Edwards, Label-free characterization of peptide-lipid interactions using immobilized lipodisks, *Anal. Chem.* 85 (15) (2013) 7377–7384.
- [36] S.J. Fraser, et al., Surface immobilization of bio-functionalized cubosomes: sensing of proteins by quartz crystal microbalance, *Langmuir* 28 (1) (2012) 620–627.
- [37] K. Hayashi, et al., Effect of dehydrocholic acid conjugated with a hydrocarbon on a lipid bilayer composed of 1,2-dioleoyl-sn-glycero-3-phosphocholine, *Colloids Surf. B: Biointerfaces* 181 (2019) 58–65.
- [38] Y. Gerelli, et al., Lipid exchange and flip-flop in solid supported bilayers, *Langmuir* 29 (41) (2013) 12762–12769.
- [39] J.E. Nielsen, et al., A biophysical study of the interactions between the antimicrobial peptide indolicidin and lipid model systems, *Biochim. Biophys. Acta Biomembr.* 1861 (7) (2019) 1355–1364.
- [40] C. Mårtensson, V. Agmo Hernández, Ubiquinone-10 in gold-immobilized lipid membrane structures acts as a sensor for acetylcholine and other tetraalkylammonium cations, *Bioelectrochemistry* 88 (2012) 171–180.
- [41] E. Madrid, S.L. Horswell, The electrochemical phase behaviour of chemically asymmetric lipid bilayers supported at Au(111) electrodes, *J. Electroanal. Chem.* 819 (2018) 338–346.
- [42] A.-S. Cans, et al., Measurement of the dynamics of exocytosis and vesicle retrieval at cell populations using a quartz crystal microbalance, *Anal. Chem.* 73 (24) (2001) 5805–5811.
- [43] R. Bordes, F. Höök, Separation of bulk effects and bound mass during adsorption of surfactants probed by quartz crystal microbalance with dissipation: insight into data interpretation, *Anal. Chem.* 82 (21) (2010) 9116–9121.
- [44] A. Vorobiev, et al., Recent upgrade of the polarized neutron reflectometer super ADAM, *Neutron News* 26 (3) (2015) 25–26.
- [45] Software pySAded, I., v1.5.2. <https://www.ill.eu/users/instruments/instruments-list/superadam/software/>, 2021 (25.05.2021).
- [46] J.F. Nagle, S. Tristram-Nagle, Structure of lipid bilayers, *Biochim. Biophys. Acta Rev. Biomembr.* 1469 (3) (2000) 159–195.
- [47] M. Björck, G. Andersson, GenX: an extensible X-ray reflectivity refinement program utilizing differential evolution, *J. Appl. Crystallogr.* 40 (6) (2007) 1174–1178.
- [48] M. Björck, Fitting with differential evolution: an introduction and evaluation, *J. Appl. Crystallogr.* 44 (6) (2011) 1198–1204.
- [49] C. Montis, et al., Nucleolipid bilayers: a quartz crystal microbalance and neutron reflectometry study, *Colloids Surf. B: Biointerfaces* 137 (2016) 203–213.
- [50] S. Tristram-Nagle, H.I. Petrache, J.F. Nagle, Structure and interactions of fully hydrated dioleoylphosphatidylcholine bilayers, *Biophys. J.* 75 (2) (1998) 917–925.
- [51] B.G. Sanganahalli, P.G. Joshi, N.B. Joshi, Differential effects of tricyclic antidepressant drugs on membrane dynamics—a fluorescence spectroscopic study, *Life Sci.* 68 (1) (2000) 81–90.